UNITED NATIONS UNIVERSITY
UNU-GTP
Geothermal Training Programme

Orkustofnun, Grensasvegur 9,
IS-108 Reykjavik, Iceland

Reports 2016
Number 18

GEOTHERMOMETRY AND QUANTIFYING OF MIXING AND WATER-ROCK INTERACTIONS IN THE NGOZI GEOTHERMAL FIELD, SW-TANZANIA

Sadock Josephat
Tanzania Geothermal Development Company
P. O Box 14801, Dar es Salaam
TANZANIA
sadockz16@gmail.com

ABSTRACT

Ngozi geothermal field is located at the southern triple junction of the East African Rift System (EARS) where the Rukwa-Tanganyika basin, the Ruaha-Mtera-Usangu segment and the Karonga-Malawi rift branches meet. Being at the triple junction the area is characterized by complex tectonic forces leading to development of structures trending in the NW, NE and NS directions. The area is characterized by the Ngozi volcano, which is one of the four volcanoes in the Mporoto-Rungwe volcanic province. Surface geology is characterized by pyroclastic ash cover while outcrops of basalts, trachy-andesite, phonolitic trachyte, alluvial sediments and sandstones occur in some parts. Geothermal surface manifestations in the area include thermal springs and altered ground and gas vents. The surface water consists of rivers, cold and warm springs, hot springs and a lake. The waters are mostly dilute (<100 ppm Cl) with the exception of the lake water that is more saline (~1500 ppm Cl) and have discharge temperatures of 30-82°C. Based on geothermometry, the maximum reservoir temperatures for the springs are ~120-130°C. Mixing model reviles that the surface thermal waters are a mixture of non-thermal water (rivers), reservoir thermal fluid, and saline lake water. Some thermal and non-thermal water show elevated CO_2 concentrations considered to originate from deep source(s). The chemistry of thermal waters shows that the concentration of main rock forming elements are controlled by water-rock interaction.

1. INTRODUCTION

Ngozi geothermal field is located in the southwest Tanzania, partly in the Mporoto Ridge Forest Reserve, which act as a hydrological divide in the area. The ridge also controls the climate of the area. The northern part of it is sparsely vegetated and warm most times of the year while the southern part has dense vegetation, rainfall and is cooler. The area is characterized by fertile soils, which have attracted intense human activities ranging from settlement, pastoralism to farming of different crops.

The area is characterized by tropical climate where dry and cold months are June to October while other months are warmer and associated with rainfall of varying quantities. High abundance of rainfall has encouraged thick vegetation in some of the prospect areas as seen in Figure 1. There is high temperature fluctuation in the area between day and nights with temperature ranging from 5 to 29°C. According to

Delalande et al. (2015), specific meteorological conditions occur within the Ngozi caldera where average annual air temperature above Lake Ngozi was 18°C with seasonal variation of ±1°C while the annual average temperature for the region is 17°C. Lake Ngozi is almost permanently covered by clouds which reduce the rate of evaporation on the lake surface.

Ngozi geothermal field has been studied by a number of academicians and researchers at different times and has been proven to have a significant geothermal resource (Kalberkamp et al., 2010; Kraml et al., 2010; Ochmann, and Garofalo, 2013; TGDC and GDC, 2015). The contribution of the present study to geoscientific knowledge of the area includes an estimation of subsurface temperatures for thermal springs around the Ngozi volcano, modelling of mixing trends of different water types in the area (lake, thermal springs and river waters) and quantification of the water-rock interactions in the area.

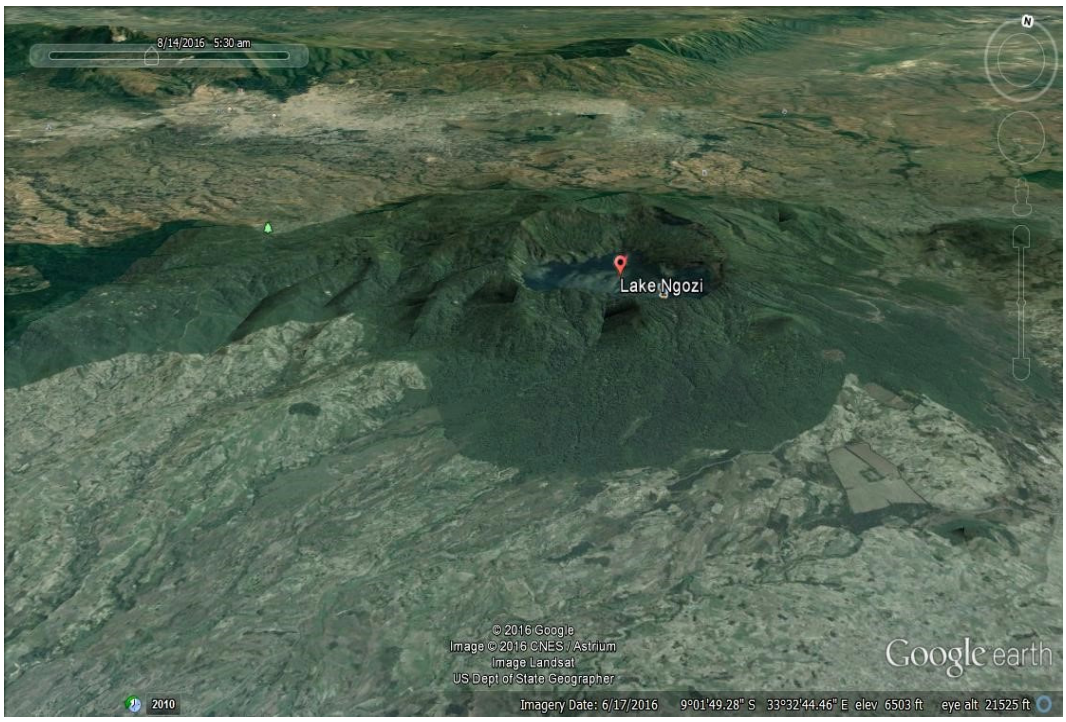

FIGURE 1: Google earth image showing topography around Lake Ngozi

2. DESCRIPTION OF THE STUDY AREA

2.1 Topography and evolution of Ngozi caldera

The topography in the Ngozi geothermal field appears to have been largely influenced by its geological setting with generally mountainous and hilly appearance, most of which are volcanic cones, domes and eruption craters (Figure 1). The Ngozi volcano marks the highest elevation in the area with the caldera rims standing at 2,260 m a.s.l. Being 2.5 km long, 1.6 km wide with a surface of about 3.1 km^2 and depth of 74 m, Lake Ngozi is considered the second largest Crater Lake in the East African Rift and Africa and it drains a watershed of 4.6 km^2 (Delalande et al., 2015).

Lake Ngozi is located inside a collapsed caldera of late Quaternary to Holocene age inside the Mporoto-Rugwe volcanic province (Fontijn et al., 2012; Delalande et al., 2015). The caldera is characterized by vertical rims, which have been collapsing over time. Landslides, soil creeping and denudation are common around the caldera rims especially on the faulted blocks (Delalande et al., 2015). The sides of the caldera are dominated by tuffs and some bands of lava all of phonolitic-trachytic and other basaltic

composition rocks (Delalande et al., 2015; TGDC & GDC, 2015). The Ngozi caldera forming eruption was previously considered to have occurred in Late Quaternary (Fontijn et al., 2012) but based on more detailed field investigation the caldera forming eruption is now considered of Holocene age (Fontijn et al., 2010a) and described as Kitulo Pumice eruption. The Ngozi tuff eruption, mostly observed south of Ngozi caldera <1 ka (Fontijn et al., 2012), reshaped the Ngozi caldera to its near present shape (Fontijn et al., 2010a).

2.2 Volcanology, surface geology and structural geology

The Mporoto-Rungwe volcanic province consists of four main volcanic eruption: Ngozi (2,260 m a.s.l.), Rungwe (3,000 m a.s.l.), Tukuyu (1,300 m a.s.l.) and Kiejo (2,200 m a.s.l.). Many other small volcanoes are likely to result from continental hot spot or plume activity (Ebinger et al., 1989; Delalande et al., 2015). Both Rungwe and Ngozi volcanoes were characterized by plinian-style of eruption in the Holocene time and magmatic activities in the area are limited to the accommodation zone between Rukwa, Malawi and Usangu Rift Basins (Fontijn et al., 2012). Ngozi had a major plinian eruption style about 10 ka ago and an ignimbrite forming eruption within the last 1 ka (Fontijn et al., 2010b).

Most of the prospect area is characterized by pyroclastic ash with outcrops of basalts, trachy-andesite, phonolitic trachyte, alluvial sediments and sandstones in some parts (Figure 2). The area was affected by tectonic forces which led to development of various geological structures like faults and lineaments. Other observed structures are series of eruption centres which are prominent in the area (TGDC & GDC, 2015). The flanks of the Ngozi volcano are covered by thick forest with few parts where volcanic ash/soil is exposed. Mass wasting processes seem to be common around the caldera despite a thick vegetation cover. A number of small undulating hills appear faintly in the horizon northwest and southeast of the volcano. Erosional channels have curved deep gullies forming a radial pattern around Ngozi which act as waterways draining the thickly vegetated volcanic flanks.

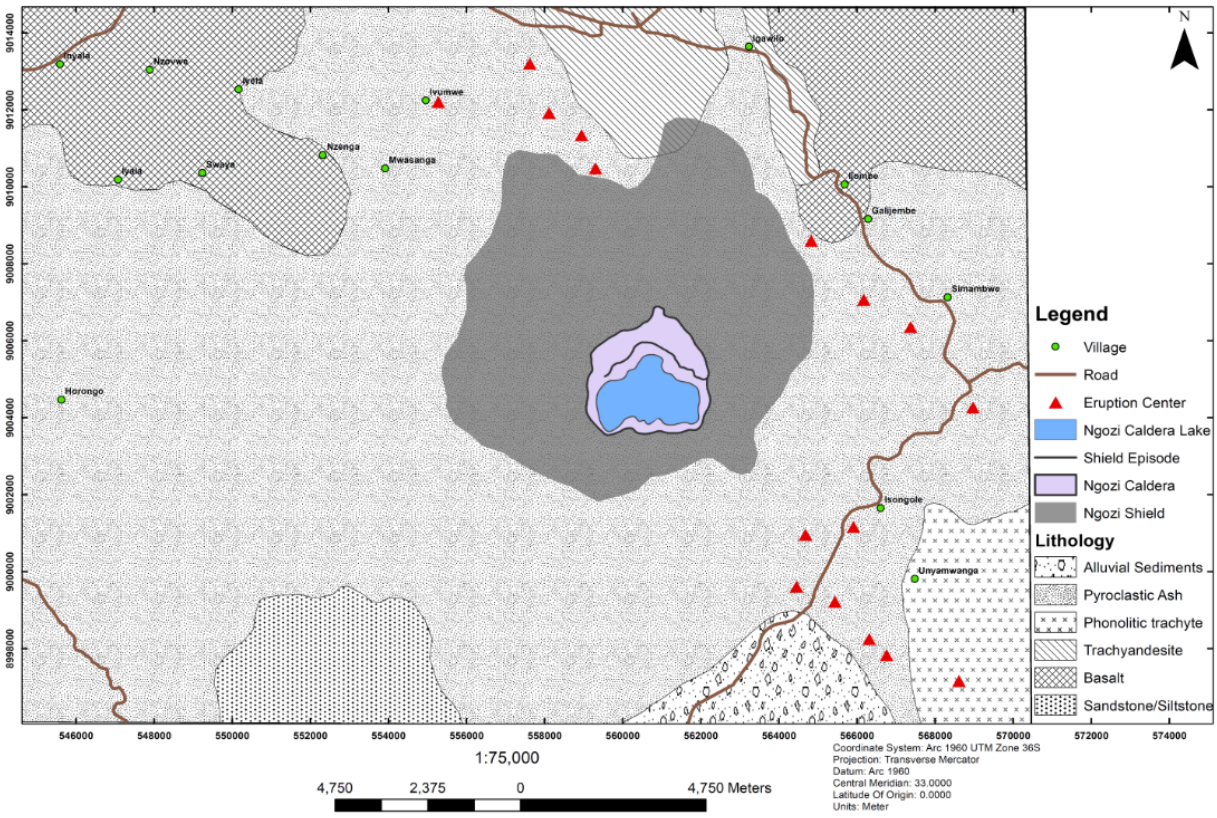

FIGURE 2: Geological map of Ngozi geothermal field (TGDC & GDC, 2015)

Surface geology at Ngozi is characterized by volcanic rocks of Plio-pleistocene to Holocene age, local low elevation areas are however filled with recent alluvial sediments. Using the Source Parameter Imaging (SPI) technique, the thickness of pyroclastic material in the area has been estimated to be at average 1000 m. This material probably forms the cap rock for the geothermal system in the area.

The heat source for the Ngozi geothermal system may be the trachytic magma chamber that was replenished during the Holocene (Kraml et al., 2010) and the event is possibly associated with the fault controlling the location of the volcano (Fontijn et al., 2010a). The geophysical survey conducted by Kalberkamp et al. (2010) concluded that the geothermal reservoir is on the NW of lake Ngozi and could be accessed by drilling 2,200 m deep wells. This is also supported by a negative Bouguer gravity anomaly correlating with the volcanic eruption centres which suggests that the heat source is located near the Usangu-Karonga accommodation zone at relatively shallow depth (Ebinger et al., 1989).

Mapping of structures in the area has been a challenge due to a thick cover of pyroclastic materials. However, several structures were mapped using remotes sensing techniques (Fontijn et al., 2010a) and field observations. The mapped structures can be grouped as lineaments, inferred faults, observed faults and alignment of eruption centres. The lineaments mapped, largely agree with the strike of regional tectonic structures in the area (Fontijn et al., 2010a) which exhibit NNE, NNW and NE trends. The NNE trending lineaments mapped east of the volcano are mimicking old basement structures (TGDC & GDC., 2015). The NW and NE lineaments appear to be following the current stress regime that reactivated NW and NE faults (Fontijn et al., 2010a) and are therefore younger. This kind of movement is expected in a region where several stresses intersect and this is true for Ngozi located at the triple junction of the regional mobile belts. The inferred faults on the east and southeast of the volcano, strike NE and NW forming several intersections with each other (Figure 3). They are inferred based on the alignment of the eruption centres from field observation. The observed faults occur to the northwest and southwest of the volcano. The downthrows of these faults are to the southeast and northeast creating a basin that pre-dates the Ngozi volcanic activity (TGDC & GDC, 2015). They are therefore bounding faults to the Ngozi geothermal system limiting the possibility of its connection with the Songwe geothermal system.

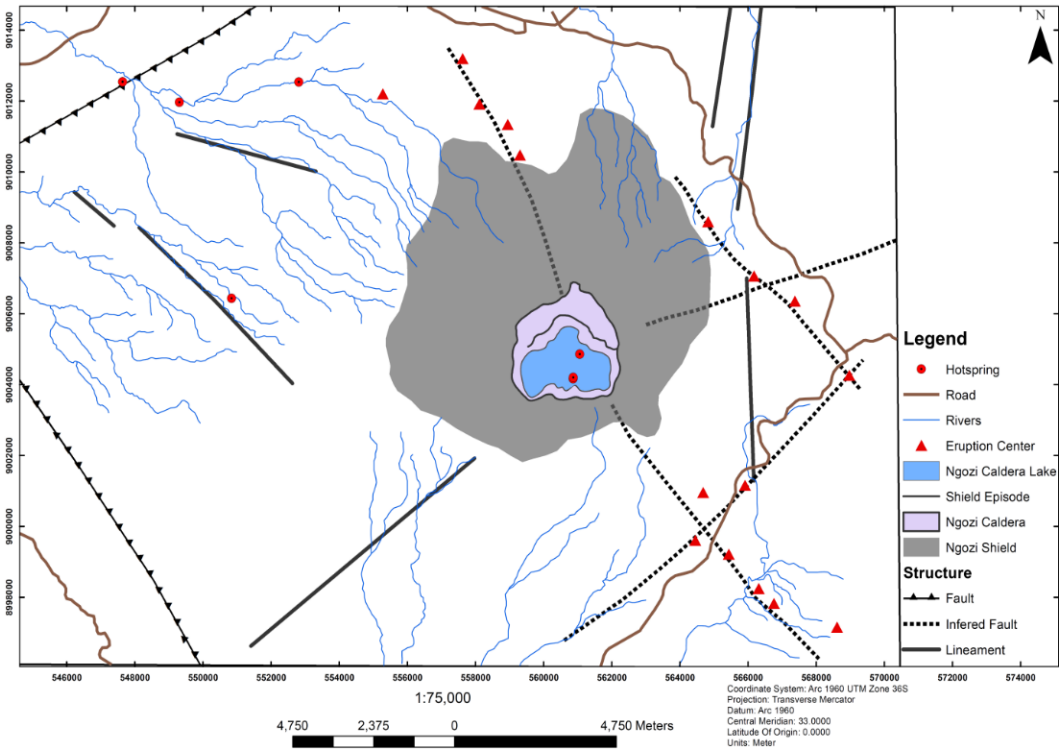

FIGURE 3: The map showing geological structures, drainage pattern and geothermal surface manifestations in the Ngozi geothermal field (TGDC & GDC, 2015)

2.3 Tectonic setting

Ngozi geothermal field is located at the triple junction of the Rukwa-Tanganyika, Usangu and Karonga-Malawi rift branches of the East African Rift System (EARS) where the Nyasa Rift split into the eastern and western braches around the stable Tanzanian Craton (Frontijin et al., 2012; Delalande et al., 2015). The western branch of the EARS in the south of Tanzania is made up by Lake Rukwa and Lake Tanganyika Rifts while the eastern branch is evidenced by the Usangu basin which trends in NE direction. The NE trending segment is poorly defined, it is punctuated by the Mtera, Ruaha and Usangu depression, but the study area is precisely located between the NW trending Rukwa-Tanganyika basin, N-S Karonga-Malawi rift basin and NE trending Usangu basin of the Ruaha-Mtera-Usangu segment (Fontijn et al., 2010a) as shown in Figure 4. The current stress regime has been interpreted by Fontijn et al. (2010a) as NE-SW compression along the NNW-SSE to N-S trending strike-slip faults.

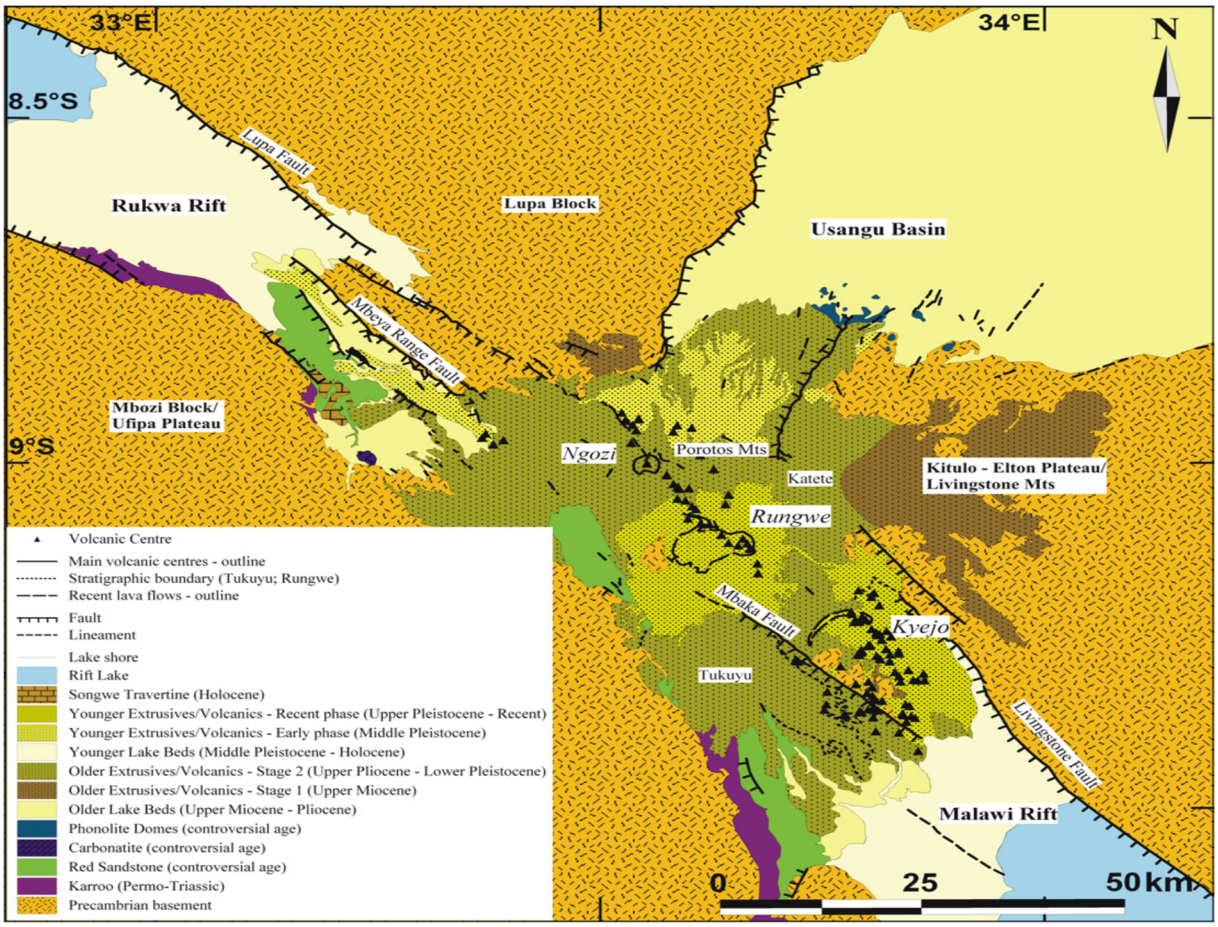

FIGURE 4: Location of the study area at the southern triple junction of the East Africa Rift System. Map taken from Fontijn et al. (2012)

The location of volcanic centres including the main volcano in the study area (Ngozi volcano) is tectonically controlled (Fontijn et al., 2010a). The Ngozi volcano is located at the intersection of active faults especially faults associated with the Usangu basin. A narrow NW-SE elongated zone of vents passes through the volcano summit and is consistent with the major NW-SE buried rift fault intersecting with NNE-SSW faults (Frontijn et al., 2012).

2.4 Hydrology

The drainage pattern of the area shows that the Mporoto ridge hosting the Ngozi caldera lake acts as a hydrological divide in the area. This is evidenced by multiple rivers draining radially away from the

volcano (Figure 3). The flow of these rivers is structurally controlled according to observation by Delvaux et al. (2010). Meteorological data shows that in the area there is more rainfall than in the other low-lying areas within the Mbeya region. Most of the rainfall at Ngozi volcano is infiltrated into the ground recharging the ground water reservoir and the deeper geothermal system (TGDC and GDC, 2015). The infiltration rates are high because evaporation and surface runoff are minimal due to the thick vegetation cover. The pyroclastic from younger eruptions ensures suitable aquifers in terms of permeability and storability below the area.

Considering the elevation of Lake Ngozi which is higher than all the nearby surroundings, recharge of the geothermal system has been considered to be local recharge by precipitation. Due to peculiar features of Lake Ngozi, it was proposed that it receives water from the geothermal reservoir below (Delalande et al., 2015). This is in agreement with the bathymetry survey results described in the next section.

2.5 Geothermal activities in the area

Geothermal activity in the area appears to be related to volcanic and plate tectonic activities which pave the way for heat, volatile and deep water uprising (Delvaux et al., 2010; Delalande et al., 2015). The hot and warm springs in the study area mainly occur in the NW and far to the SE of the Ngozi volcano and are attributed to the ascent of magmatic fluids (Delalande et al., 2011). Most thermal springs are aligned along the major NW-SE rift trend controlled by the development of the Rukwa and North Nyasa rift basins (Delvaux et al., 2010).

Geothermal surface manifestations are limited in the area, the visible surface manifestations include hot and warm springs, CO_2 vents and young volcanic eruption centres including calderas (Njue, 2015). Surface manifestations are believed to have been masked by a thick volcanic ash cover hence Ngozi can be described as an almost blind geothermal system. This volcanic ash cover is the result of plinian-style volcanic eruption that affected the area during the Holocene (Fontijn et al., 2012). The hot and warm springs of temperatures up to 30 - 82.4°C occur in low elevation, NW of Ngozi volcano. The cold CO_2 vents in the area includes the Shiwaga crater in the southeast of Ngozi volcano and CO_2 vent bubbling into Shiwaga River in the southwest of the Ngozi volcano. Frontijn et al. (2012) proposed that these gas vents imply the presence of magma at depth. Gas chemistry determination has proved that the helium and CO_2 characterizing the area are of mantle origin (de Moor et al., 2012). Due to limited geothermal surface manifestations, efforts have been employed to search for geothermal indicators that may not be directly visible at the surface. Here discussed are a bathymetry survey and sampling of rocks and lithics of the volcanic cones, crater and marls. Bathymetric survey was conducted by the Federal Institute of Geosciences and Natural Resources of Germany (BGR) in collaboration with expertise of the Ministry of Energy and Minerals of Tanzania, the Geological Survey of Tanzania and Tanzania Electric Supply Company. The survey results revealed three hot spring feeding the Ngozi caldera lake from below.

According to Ochmann and Garofalo (2013), two hot springs discharging 78°C and 89°C hot water exist south of the lake while one hot spring discharging 66°C hot water is on the north bank of the lake. These hot springs are aligned on a N-S trending line, implying that their locations is structurally controlled (TGDC & GDC, 2015). During January 2016, fieldwork samples of rocks fragments and lithics were collected from different eruption centres including volcanic cones, domes and marls for XRD and microscopic analysis. XRD analysis identified different type of clay including illite, smectite and kaolinite. The presence of illite indicates that the samples were once in the reservoir environment at temperature >200°C, also this assemblage of secondary minerals indicate hydrothermal alterations in the area. Petrographic analysis identified secondary minerals like calcite, clays, epidotes, quartz, and zeolites. These secondary minerals suggest that the sampled rocks has been in reservoir conditions.

3. METHODOLOGY

3.1 Water sampling and analysis

Sampling and analysis were conducted in the course of studies that took place in the Ngozi geothermal field at different times. For the lake water samples were collected on the lake surface and measurements for temperature, pH, EC and TDS were made along vertical profiles. In the recent geochemical study, carried out by TGDC in collaboration and GDC and UNEP in January 2016, samples collection and treatment was done according to the procedures described by Nicholson (1993). Samples for determination of pH, TDS, conductivity and total carbonate were not treated. Samples for anions analysis were only filtered using 0.45 µm filter membrane, samples for analysis of cations were filtered and acidified by 1 ml HCl. Samples for SiO_2 analysis were diluted to avoid silica polymerization while 1 ml of 0.2 M Zn-acetate was added to samples for SO_4 analysis in order to precipitate sulphur as zinc sulphide (ZnS).

Analysis of H_2S was done on site by titration using 0.1M HCl and 0.001M mercuric acetate ($C_4H_6O_4Hg$), also measurement of pH, TDS and EC were done in the field using a pH/TDS/conductivity meter. Laboratory analysis of samples was conducted in the GDC laboratory. Analysis of B, SiO_2 and SO_4 was done with the spectrophotometry method using UV-Vis, analysis of Na, K, Ca, F and NH_4 was done with the electrochemical method using ISE while analyses of Mg, Cl and TCC-CO_2 were done by using EDTA, Mohr's titration and autotitrator respectively. A total number of 70 water analyses from the lake, thermal springs and rivers were considered for this study.

3.2 Speciation, ionic balance calculations and water-rock interaction

Speciation, ionic balance also referred to as charge balance calculation and calculation of reaction quotient (Q) and equilibrium constants (K) values used for evaluation of water-rock interaction was done by using the WATCH 2.4 computer program (Bjarnason, 2010). Ionic balance was calculated in order to check the quality of data before proceeding to data processing and interpretation. Although it was applied here, CBE has received some critiques including that it takes into account the major charged ions leaving behind the neutral species and trace components (Nicholson, 1993; Arnórsson, 2000). Data with ionic/charge balance of -10% to 10% (Figure 5), which are considered good (Arnórsson, 2000), were only 44 hence further processed in this study.

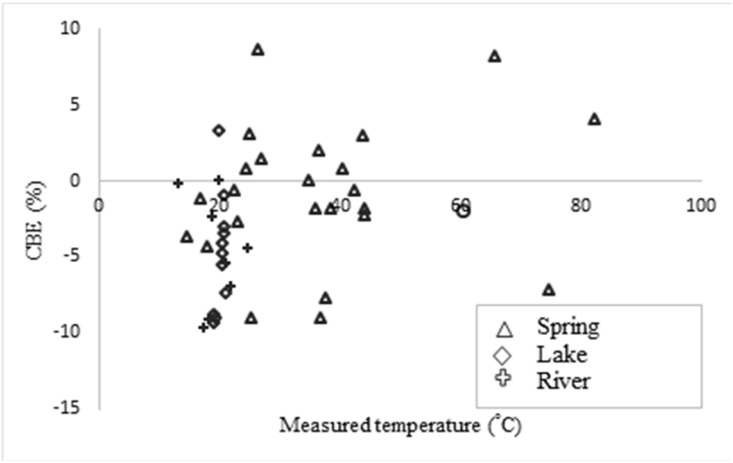

FIGURE 5: Ionic balance for the data used in this study

The log Q and log K values were used to calculate the saturation indices (SI) of the waters in respect to secondary minerals using equation 1. This calculation was performed using excel and the minerals selected were anaclcime, chalcedony, laumontite, Na-montmorillonite, K-montmorillonite and Ca-montmorillonite. The SI values were then used to assess if waters under investigation were under saturated, saturated or super saturated in respect to the secondary minerals.

$$SI = logQ - logK \quad (1)$$

where Q is the reaction quotient and K is the reaction equilibrium constant.

3.3 Geothermometry calculation

Geothermometry refers to the use of chemical composition of thermal fluids to estimate the subsurface (reservoir) temperature. There are different Geothermometry techniques used, among others solute, gas, isotope and multiple equilibrium geothermometry. Solute geothermometers are based on temperature dependent mineral-fluid equilibria. Solute geothermometers includes SiO_2, Na/K, Na-K-Ca, Na-K-Ca (Mg-correction), Na/Li, K/Mg, Li/Mg, Na-K-Mg, Ca/Mg and SO_4/F (Fournier and Potter, 1979; Marini et al., 1986; Nicholson, 1993).

In this study, multiple equilibrium geothermometry technique was adopted to constrain the aquifer temperatures for thermal springs around the Ngozi volcano. Four thermal springs (Inyala, Ikumbi, Shongo and Ilamba) were selected for geothermometry calculation. This technique was adopted because it provides good temperature estimates and it does not involve assumption of particular fluid-mineral equilibria to exist in the subsurface as it is the case for other conventional geothermometers (Reed and Spycher, 1983; 1984). This technique involves to simultaneously look at the saturation state of different minerals and to find the mineral suites that are likely to equilibrate with water (Reed and Spycher, 1984).

The estimation of aquifer temperatures involves plotting of log (Q/K), which is the saturation index, as a function of temperature and assessment of the intersection of the curves. The saturation states of different minerals were calculated using the PHREEQC Version 3 computer program (Parkhurst and Appelo, 2015). For comparison purposes, other solute geothermometers were also used to estimate the subsurface temperature for Inyala, Ikumbi, Shongo, and Ilamba thermal springs. The geothermometers used are quartz, chalcedony, Na-K-Ca (Mg-correction) and K/Mg and their equations are presented in Table 1.

TABLE 1: Solute geothermometry equations used in this study

Geothermometers	**Equation**	**Source**
Quartz	$t(°C) = C_1 + C_2S + C_3S^2 + C_4S^3 + C_5 logS$	Fournier and Potter, 1982
Chalcedony	$t(℃) = \frac{1032}{4.69 - logS} - 273.15$	Fournier, 1977
Na-K-Ca (Mg correction)	$t(℃) = \frac{C_{Mg}}{C_{Mg} + 0.6C_{Ca} + 0.31C_K} \times 100$	Fournier and Potter, 1979
K/Mg	$t(℃) = \frac{4410}{13.95 - L_{km}} - 273.2$	Giggenbach, 1986

C_1 = -4.2198 x 10^1, C_2 = 2.8831 x 10^{-1}, C_3 = -3.6686 x 10^{-4}, C_4 = 3.1665 x 10^{-7}, C5= 7.7034 x 10^1, S=Concentration of SiO_2, C = Concentration, $L_{km} = logC_{K+}^2/C_{Mg2+}$

3.4 Modelling of mixing

The process of quantifying mixing in this study was based on the chloride-enthalpy mixing model developed and described by Björke et al. (2015) and Stefánsson et al. (2016). The only modification made to this model in order to fit the current study is that temperature was replaced by SiO_2 concentration. The end members water types defined for quantifying mixing in this study are lake water (lk), thermal spring waters (spr) and river waters (riv). The sample with highest chloride among the analyses of lake water was chosen to represent lake water, Inyala was chosen to represent thermal springs and the Mbalizi River was chosen to represent rivers as non-thermal waters in this study. Results of mixing calculations presented in Table 2 were done using the factor D defined by the mathematical equations presented below by applying Cramer's rule.

TABLE 2: Percentage mixing between lake, thermal spring and non-thermal waters in Ngozi geothermal field

Sample location	X^{lk}	X^{spr}	X^{riv}
Thermal springs waters			
Ilamba	0.000*	0.236	0.766
Manyogopa	0.000*	0.065	0.935
Mbete	0.000*	0.005	0.995
Ivumwe	0.002	0.434	0.570
Mwasanga	0.006	0.125	0.878
Hombo	0.001	0.186	0.816
Ibayi	0.074	0.382	0.655
Songwe	0.129	0.250	0.812
Udindilwa	0.053	0.289	0.738
Songwe	0.130	0.254	0.809
Aqua Afia	0.000*	0.852	0.155
Aqua Afia	0.000*	0.947	0.061
Ikumbi	0.000*	0.873	0.134
Ikumbi	0.000	0.862	0.145
Inyala	0.000	1.000	0.008
Iyela	0.002	0.915	0.094
Shimilaa	0.003	0.431	0.574
Shongo	0.000*	0.895	0.111
Swaya	0.005	0.470	0.536
Swaya	0.005	0.485	0.521
Inyala	0.004	0.980	0.030
Shongo	0.000	0.869	0.139
Lake water			
Ngozi	0.941	0.000*	0.059#
Ngozi	0.952	0.000*	0.048#
Ngozi	0.977	0.000*	0.023#
Ngozi	0.967	0.000*	0.033#
Ngozi	0.981	0.000*	0.019#
Ngozi	1.000	0.000	0.000#
Ngozi	0.984	0.013	0.003#
Ngozi	0.975	0.005	0.020#
Ngozi	0.970	0.019	0.012#
Ngozi	0.966	0.013	0.021#
Ngozi	0.988	0.000*	0.012#
Ngozi	0.973	0.000*	0.027#
River waters			
Mchewe	0.000	0.000*	1.000#
Igogwe	0.165	0.321	0.514#
Songwe	0.000	0.051	0.949
Shiwaga	0.000	0.139	0.862
Gogozimba	0.018	0.288	0.723
Itembele	0.000	0.254	0.748
Kiwira	0.026	0.186	0.827
Kwamana	0.015	0.253	0.756
Mbalizi	0.000	0.000	1.000
Shiwaga	0.001	0.149	0.852

* Negative values assigned to be zero

corrected values assuming $x^{lk} + x^{spr} + x^{riv} = 1$

$$D = m_{cl}^{lk}\left(SiO_2^{spr} - SiO_2{}^{riv}\right) - SiO_2^{lk}\left(m_{cl}^{spr} - m_{cl}^{riv}\right) + \left(m_{cl}^{spr}SiO_2^{riv} - m_{cl}^{riv}SiO_2^{spr}\right) \quad (2)$$

$$D^{lk} = m_{cl}^{m}\left(SiO_2^{spr} - SiO_2^{riv}\right) - SiO_2^{m}\left(m_{cl}^{spr} - m_{cl}^{riv}\right) + \left(m_{cl}^{spr}SiO_2^{riv} - m_{cl}^{riv}SiO_2^{spr}\right) \quad (3)$$

$$D^{spr} = m_{cl}^{lk}\left(SiO_2^{m} - SiO_2^{riv}\right) - SiO_2^{lk}\left(m_{cl}^{m} - m_{cl}^{riv}\right) + \left(m_{cl}^{m}SiO_2^{riv} - m_{cl}^{riv}SiO_2^{m}\right) \quad (4)$$

$$D^{riv} = m_{cl}^{lk}\left(SiO_2^{spr} - SiO_2^{m}\right) - SiO_2^{lk}\left(m_{cl}^{spr} - m_{cl}^{m}\right) + \left(m_{cl}^{spr}SiO_2^{m} - m_{cl}^{m}SiO_2^{spr}\right) \quad (5)$$

It follows then:

$$X^{lk} = D^{lk}/D \quad (6)$$

$$X^{spr} = D^{spr}/D \quad (7)$$

$$X^{riv} = D^{riv}/D \quad (8)$$

where m_{Cl} stands for chloride concentration, SiO_2 for silica concentration, m for measured value and X for fraction composition.

The Grapher 12 computer program and Excel were used to make the ternary plots showing the mixing percentages for lake, thermal spring and river waters.

4. RESULTS AND DISCUSSION

4.1 Analytical results

Ionic balance calculation results were used to select good data used in this study. Chemical relationships between the lake, thermal spring, and river waters were assessed using plots of concentration versus measured temperature for selected chemical species (Figure 6). As listed in Table 3, springs have discharge temperatures ranging from 17 to 82°C, pH from 5.82 to 6.7 and E.C from 78 to 3700 µS/cm. River waters have temperatures from 13.3 to 23°C, pH from 5.24 to 8.4 and E.C from 168 to 1350 µS/cm. Lake water has temperatures from 19.2 to 21°C, pH of 6.4 to 7.15 and E.C of 4490 to 5300 µS/cm. Lake water displays highest chloride concentration of 1505 mg/kg, high SO_4 and low CO_2 compared to most springs. Others are significantly high SiO_2, high sodium and highest potassium compared to most springs and river waters (Figure 6). The low content of SiO_2 could be a result of dilution of geothermal water by the cold lake water, low CO_2 could be a result of steam loss and high SO_4 could be a result of H_2S and/or SO_2 oxidation at the near surface when thermal water mixes with lake water while lowest magnesium could indicated little input of local ground water into the lake.

Thermal spring waters are characterized by variable characteristics (Figures 6) but are generally low in chloride, high in CO_2 and SiO_2, have moderate to high sodium, potassium varies from low to high, calcium is low, magnesium is high and sulphate content of significant to high concentrations. High magnesium levels can be a result of mixing with ground water while sulphate can be a result of reactions in the near surface to surface environment.

River waters generally display the following chemical properties (Figures 6); low chloride, sodium and potassium, low CO_2 except Shiwaga River which is associated with a cold gas vent, significant content of SiO_2 and low calcium, magnesium and sulphate. The Igogwe River displays significant amounts of both chloride and CO_2, while it has low sodium and potassium concentration because these minerals have probably reacted on the way from the lake and thermal springs to the sampling point. Other rivers display insignificant amount of lake water. Presence of lake water in the rivers was thought to be the evidence that these rivers drain the lake Ngozi water in the subsurface.

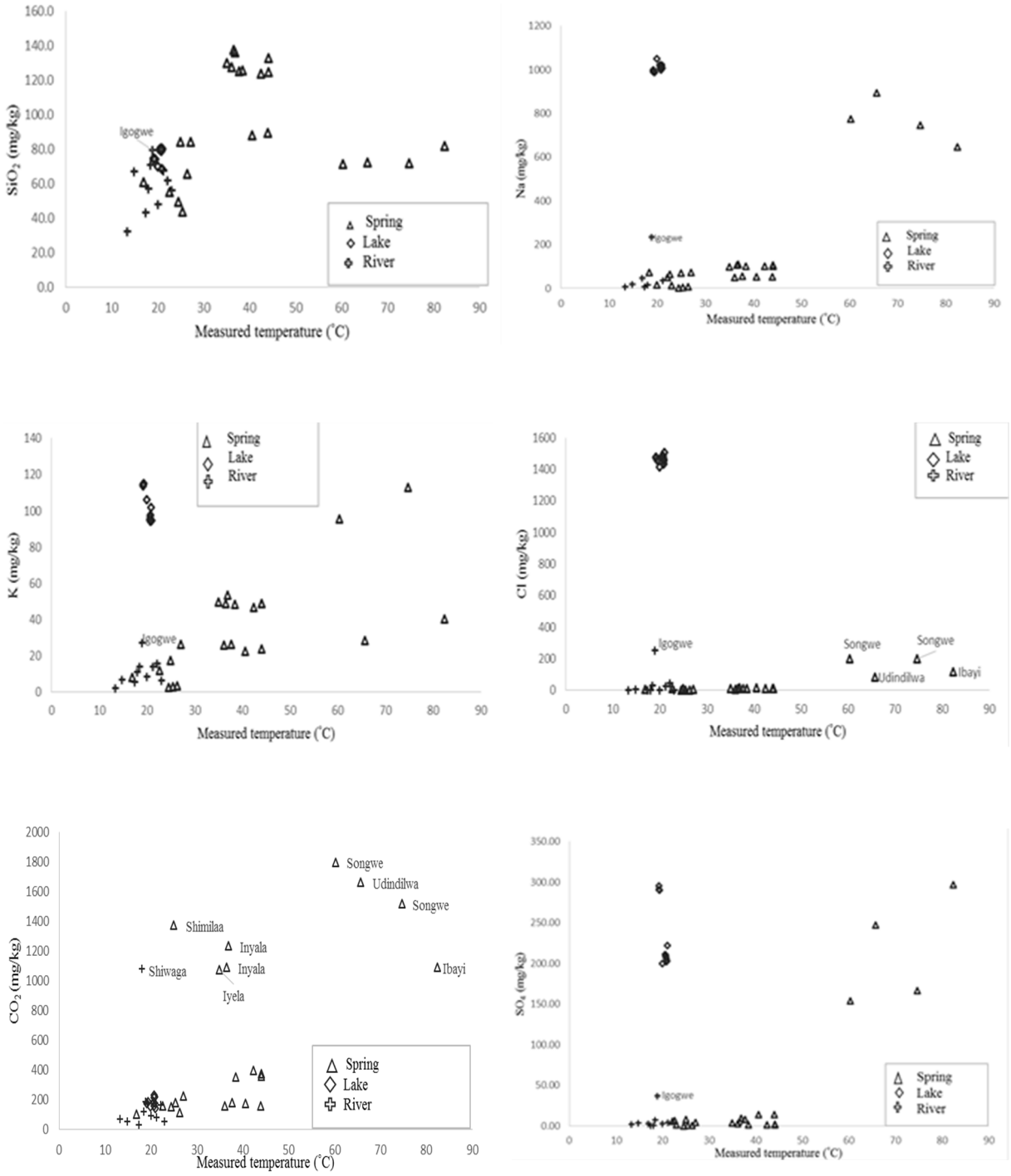

FIGURE 6: Relationship between the waters in the study area using selected chemical constituents

TABLE 3: Major chemical composition of waters in the Ngozi geothermal field, temperature (°C), EC (μS/cm), concentration in mg/kg and isotopes in ‰

		Concentrations												Isotopes	
Location	**T**	**EC**	**pH**	**SiO_2**	**B**	**Na**	**K**	**Ca**	**Mg**	**Cl**	**CO_2**	**SO_4**	**F**	**δ^2H**	**$\delta^{18}O$**
Spring water															
Ilamba	26	239	7.2	65.7	n.a	6.3	3.4	22.2	11.9	0.72	110	0.7	0.2	-22	-4
Manyogopa	25	78	5.8	49.5	n.a	2.5	2.5	5.5	4.1	0.02	149	<dl	0.1	-23	-4.1
Mbete	25	94	5.8	43.9	n.a	4.3	2.8	5.1	4.8	0.4	178	0.3	0.12	-27	-4.5
Ivumwe	27	440	6.90	84.6	0.01	71.4	26.5	5.6	4.0	7.8	223	4.2	1.95	-35.2	-6.1
Mwasanga	23	200	7.00	55.5	0.01	64.2	11.7	3.1	1.9	10.8	156	6.3	1.5	-36.8	-6.4
Hombo	17	200	8.20	61.1	0.02	47.9	8.0	2.3	1.1	4.6	100	2.8	1.2	-37.9	-6.6
Ibayi	82	2640	6.80	82.3	1.63	646.0	40.3	12.0	2.3	116	1089	297.0	<dl	-37.9	-6.1
Songwe	60	3700	6.70	71.8	0.61	775.0	95.4	30.3	15.6	197	1796	154.0	<dl	-37.1	-6.4
Udindilwa	66	3400	7.00	72.7	0.30	893.0	28.5	13.4	3.9	82.4	1659	247.0	<dl	-41.1	-6.7
Songwe	75	3580	7.2	72.2	0.17	745.4	113.0	20.9	15.6	199	1517	166.4	7.7	n.a	n.a
Aqua Afia	42	650	6.70	124.0	n.a	100.0	46.9	15.5	5.8	8.2	393	1.0	1.05	-39.6	-5.7
Aqua Afia	44	640	6.90	133.0	0.01	106.0	48.7	12.1	4.5	9	358	1.7	0.83	-38.9	-5.8
Ikumbi	39	670	7.00	126.0	n.a	102.0	48.3	15.5	5.7	8.3	351	0.9	1.08	-39.9	-5.9
Ikumbi	44	670	6.80	125.0	n.a	102.0	48.7	13.5	4.9	8.7	374	1.4	0.83	-39.4	-5.7
Inyala	37	1000	6.10	138.0	0.01	107.0	48.9	50.7	26.8	9.5	1089	4.0	0.56	-37	-6.3
Iyela	35	980	6.10	130.0	0.02	99.2	49.8	50.9	26.2	11.9	1075	3.4	0.66	-37.8	-6.6
Shimilaa	25	380	5.40	84.3	0.00	68.9	17.4	4.7	2.2	9.5	1370	8.2	0.86	-35.9	-6.3
Shongo	36	340	7.40	128.0	n.a	49.0	26.0	9.0	2.9	4.4	158	2.5	0.39	-35.4	-5.8
Swaya	41	380	6.80	88.1	0.00	51.7	22.4	11.3	4.6	12.8	175	13.9	0.46	-32.5	-5.9
Swaya	44	360	7.20	89.5	0.01	52.1	23.8	13.1	4.8	12.5	154	14.0	0.43	n.a	n.a
Inyala	37	975	6	136.3	0.40	109.0	53.4	43.9	13.3	14.7	1231	9.0	0.56	n.a	n.a
Shongo	38	325	7.1	125.6	0.70	54.9	26.2	7.7	1.1	8.8	176	8.1	0.28	n.a	n.a
Lake water															
Ngozi	20	4820	7.15	70.1	1.40	1050	106	4.2	0.9	1416	149	200.00	<dl	n.a	n.a
Ngozi	21	5300	6.70	68.7	1.41	1020	102	3.8	0.9	1433	178	203.00	6.49	-10.7	-1.4
Ngozi	19	4670	6.7	75.1	n.a	991	115	3.9	1	1470	178	291.00	8	-11	-1.4
Ngozi	19	4690	6.7	74.2	n.a	987	115	3.8	0.9	1456	184	290.00	7	-11	-1.3
Ngozi	19	4690	6.7	74.2	n.a	1000	114	3.9	0.9	1477	172	295.00	7	-12	-1.3
Ngozi	21	4510	6.8	80.2	n.a	1008	94.8	3.9	0.9	1505	138	222.30	12.4	-10	-1.2
Ngozi	21	4500	6.5	80.9	n.a	1018	96.2	3.9	0.9	1481	156	16.68	12.0	-11	-1.4
Ngozi	21	4500	6.4	79.8	n.a	1009	94.4	3.9	0.9	1468	226	16.46	11.9	-10	-1.3
Ngozi	21	4490	6.4	80.9	n.a	1021	94.5	3.9	0.9	1460	217	203.20	11.5	-11	-1.2
Ngozi	21	4490	6.4	80.2	n.a	1000	95.2	3.9	0.9	1455	179	16.55	11.8	-12	-1.4
Ngozi	21	4510	6.4	79.6	n.a	1022	95.1	4	0.9	1487	195	16.42	12.1	-10	-1.4
Ngozi	21	4510	6.4	79.2	n.a	1015	97.6	34	0.9	1464	209	202.30	12.1	-10	-1.4
River water															
Mchewe	13	168	8.40	32.4	<dl	8.2	2.0	16.2	5.9	0.4	72	1.6	0.18	-37.5	-6.4
Igogwe	19	1350	8.20	79.9	0.24	234.0	27.3	12.8	9.6	252	186	36.5	9.05	-28.7	-5.1
Songwe	20	200	8.00	48.3	0.02	16.6	8.6	14.4	6.4	1.9	91	2.7	0.49	-33.1	-5.4
Shiwaga	23	200	6.90	56.6	0.00	14.1	6.5	3.3	1.3	2.3	55	1.0	0.35	-30.6	-5.6
Gogozimba	18	358	7.9	71.3	n.a	73.0	13.8	2.1	1.1	30	118	7.0	9.05	-34	-5.5
Itembele	15	109	7.5	67.5	n.a	18.7	6.8	5.0	1.3	3.08	53	3.1	0.73	-35	-5.6
Kiwira	22	334	6.4	62.0	n.a	49.6	15.6	3.8	3.0	42	164	5.6	1.93	-33	-5.5
Kwamana	21	184	8.1	67.9	n.a	35.0	14.0	7.0	3.9	26	80	4.4	0.56	-38	-6
Mbalizi	17	55	7.4	43.4	n.a	7.7	5.3	1.9	0.8	0.8	29	0.5	0.24	-39	-6.1
Shiwaga	18	110	5.2	57.5	n.a	14.8	10.9	9.3	3.8	3	1082	0.8	0.2	-29	-5.6

n.a = not analysed
<dl= below detection limit

4.2 Classification of waters

In this study classification of waters was done using the Cl-SO_4-HCO_3 and Na+K-Ca-Mg ternary diagrams. The Cl-SO_4-HCO_3 ternary diagram classify the geothermal waters on the basis of the abundance of major anions. In Figure 7, Lake Ngozi water plots close to the field of mature water (Cl vertex) while the thermal springs plot close to the field of peripheral water (HCO_3 vertex).

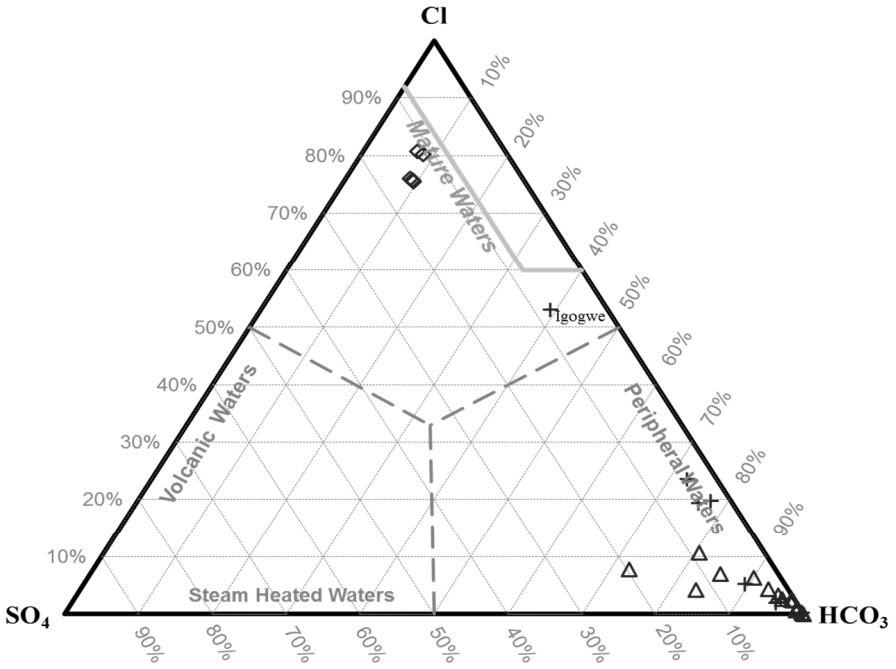

FIGURE 7: A Cl-SO_4-HCO_3 ternary plot showing classification of waters in the Ngozi geothermal field. Diamond shapes represent lake water, triangles thermal spring waters and crosses river waters

The chemistry of river waters depends on the mixing of lake and thermal spring waters. Most rivers plot in the HCO_3 field which can be interpreted as a result of heavy mixing with thermal spring waters. The Igogwe River has a significant amount of Lake Ngozi water hence it plots close to the lake water.

In Figure 8, Lake Ngozi water plots at the Na + K vertex, most thermal springs plot close to the Na + K vertex while three thermal spring plot in the Ca-Mg field. River waters also plot close to the Na + K vertex as they are mixed with lake and thermal spring waters.

From this classification, it can be concluded that lake waters are of Na - Cl type and thermal spring waters are of Na - HCO_3 type. Ilamba, Manyogopa and Mbete springs are heavily mixed with non-thermal ground waters hence display Ca (Mg) - HCO_3 composition.

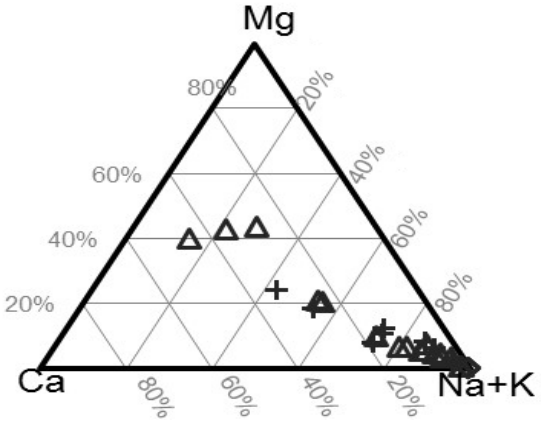

FIGURE 8: The Na+K-Mg-Ca ternary diagram showing classification of waters in the Ngozi geothermal field. Diamond shapes represent lake water, triangles thermal spring waters and crosses river waters

The geothermal brine feeding Lake Ngozi could come from the deep geothermal reservoir which is associated with magmatic gases like Cl, H_2S, SO_2 and CO_2 from a deep degassing magmatic body. This brine was not studied in detail in this work. The HCO_3 waters of thermal springs can be a result of a degassing magmatic body from where CO_2 find its way to the surface through the deep structures and mix with thermal waters. In springs fed by shallow circulation of meteoric water, HCO_3 can be a result of dissolution of carbonate bearing rocks in the area.

4.3 Geothermometry

In this study, four thermal springs namely Inyala, Ikumbi, Shongo and Ilamba were selected from the Ngozi geothermal field based on their chemistry and their subsurface temperatures were estimated. The log (Q/K) versus temperature plots that were used to estimate the subsurface temperatures for these thermal springs are presented in Figures 9-12. According to Reed and Spycher (1983), the temperature at which the log (Q/K) curves intersect each other at a saturation index (SI=0) is the equilibration temperature. Reed and Spycher (1984) described that the characteristic convergence of log (Q/K) curves for the equilibrium assemblage to zero at the temperature of equilibration establishes the basis for determining a mineral assemblage and temperature of equilibration of natural geothermal waters, fluid inclusions, hot spring waters etc. from analysis of water alone. Reed and Spycher (1984) also point out that the plots of log (Q/K) behaviour can be used to assess boiling, mixing and lack of equilibrium.

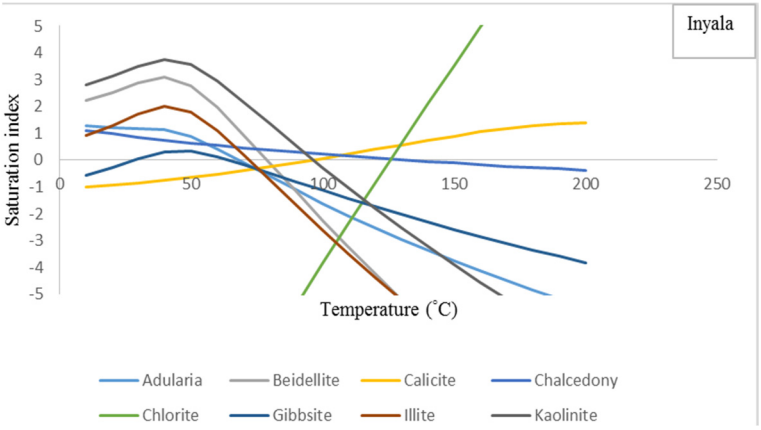

FIGURE 9: Multiple equilibrium geothermometry plot for Inyala thermal spring

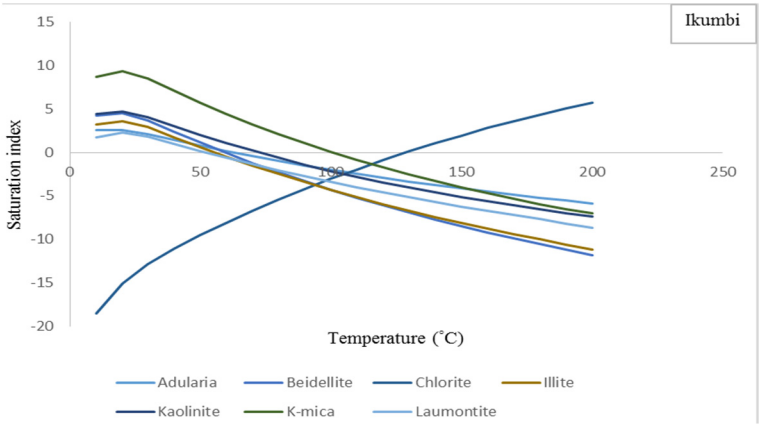

FIGURE 10: Multiple equilibrium geothermometry for Ikumbi thermal spring

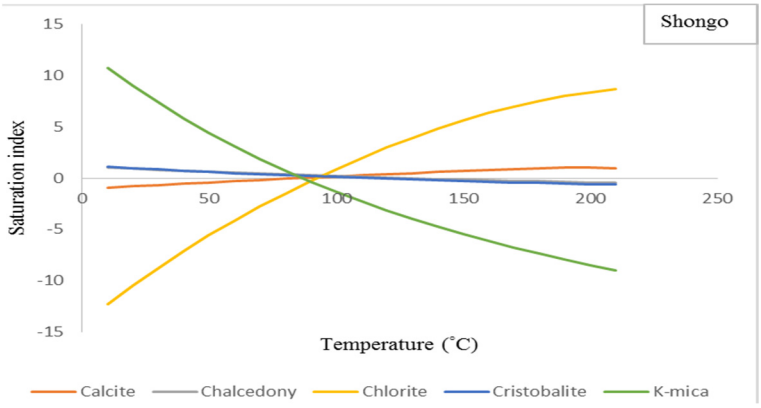

FIGURE 11: Multiple equilibrium geothermometry plot for Shongo thermal spring

For Inyala thermal spring there is no single convergent temperature as can be seen on Figure 9, the curves for adularia, beidellite, gibbsite and illite intersect the equilibrium line at the lowest temperature of about 70-80°C, calcite and kaolinite curves intersect the equilibrium line at 100°C and chalcedony and chlorite curves intersect the equilibrium line at about 125°C. Therefore, the subsurface temperature for Inyala spring can be estimated to be 70-125°C. For Ikumbi thermal spring (Figure 10), adularia, beidellite, illite, kaolinite and laumontite curves converge at 60-80°C, K-mica and chlorite intersect the equilibrium curve at 100°C and 130°C respectively, the subsurface temperature can therefore be estimated in the range of 60°C to 130°C. For Shongo spring Figure 11, K-mica, chlorite, cristobalite, chalcedony and calcite converge and intersect the equilibrium line at 85-100°C. For Ilamba spring (Figure 12) calcite, chalcedony, gibbsite and

illite converge and intersect the equilibrium line at 70-80°C. In this plot calcite has two intersections, it also converges and intersects with kaolinite and quartz at 100°C hence the temperature for Ilamba spring can be estimated to be 70-100°C.

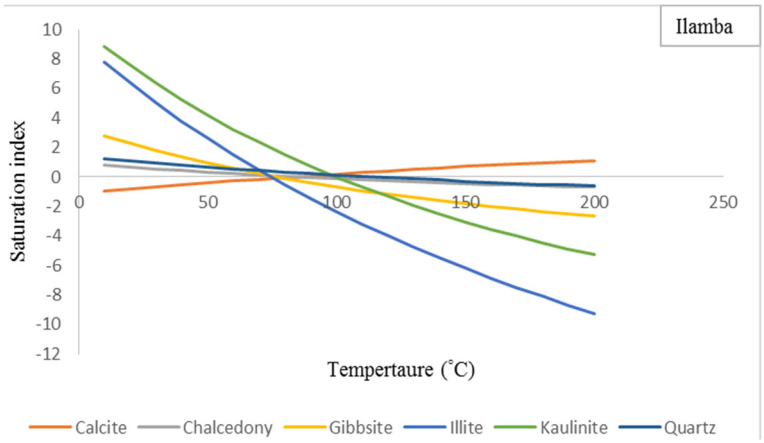

FIGURE 12: Multiple equilibrium geothermometry plot for Ilamba thermal spring

As pointed out earlier, in multiple equilibrium geothermometry technique the temperature at which the log (Q/K) curves converge and intersect the equilibrium line (SI=0) is the subsurface temperature, but most of the springs studied have no single convergence temperature. As seen from Figures 9, 10, 11 and 12, only Shongo spring display a small range of convergence temperatures, others shows a wide range of temperature which limit the probability of estimating the true temperature because the distinct clustering of the curves for many minerals in a short temperature range gives high probability that the estimated temperature is correct (Reed and Spycher, 1984). The dispersion and broadness of the log (Q/K) curves has been explained by Reed and Spycher (1984) as a possible result of water and/or CO_2 loss and/or mixing, resulting in changes concentration of components and pH changes. The convergence points for the springs has also moved down the equilibrium line which has also been explained by Reed and Spycher (1984) to be a result of mixing with near surface waters. Therefore, it was necessary to quantify the mixing processes affecting the thermal springs in the study area.

However, lack of single convergence temperature can also be a consequence of other issues like poor water analysis, poor thermodynamic data and lack of eqilibrium for a particular spring (Reed and Spycher, 1984). Analysis of the geothermometry plots also reveal that different mineral curves have different slopes, this can be interpreted as a consequence of difference in temperature sensitivity of minerals. The minerals with high slope are highly sensitive to temperature changes while the minerals with low slopes are less sensitive to temperature changes.

For comparison, other solute thermometers were also used to estimate the subsurface temperatures for the selected thermal springs and the results are presented in Table 4. Chalcedony, K/Mg and Na-K-Ca with Mg correction give fairly comparable temperatures to the multiple equilibrium geothermometry results while quartz geothermometer gives generally temperatures of about 20°C higher.

TABLE 4: Temperature estimated by different geothermometry techniques for selected springs around the Ngozi volcano in the Ngozi geothermal field

Spring	**Multiple equilibrium geothermometers (Reed and Spycher, 1983 and 1984)**	**T_chalcedony (Fournier, 1977)**	**T_quartz (Fournier and Potter, 1982)**	**T_K/Mg (Giggenbach, 1986)**	**T_Na-K-Ca (Mg corr) Fournier and Potter, 1979**
	(°C)	**(°C)**	**(°C)**	**(°C)**	**(°C)**
Inyala	80-120	132	156	116	125
Shongo	70-110	126	151	100	98
Ikumbi	70-140	125	151	120	139
Ilamba	80-100	86	115	81	62

4.4 Mixing

The composition and temperature of geothermal fluids does not remain unchanged as it ascends from the geothermal reservoir to the surface, the changes can be a result of depressurization boiling, conductive heat loss and/or mixing with cold near surface or surface water (Fournier, 1977; Reed and Spycher, 1984; Arnórsson, 1985; Arnórsson, 2000; Björke et al., 2015; Stefánsson, 2016). On ascent to the surface waters can re-equilibrate, depending on different factor like flow rate, the flow path, initial reservoir temperature and kinetics of chemical reactions taking place (Fournier, 1977). Mixing which is the subject of this section occurs when the ascending geothermal fluids meet the shallow ground or surface water sometimes referred to as dilution (Arnórsson, 1985; Arnórsson, 2000). Evaluation of mixing and reactions occurring in the up flow is important in order to understand the subsurface conditions, evaluate potential geothermal utilization and assess the environmental impacts that can arise upon extraction of geothermal fluids (Truesdell and Fournier, 1977; Arnórsson, 1985; Stefánsson et al., 2016).

The thermal springs in the study area are characterized by relatively high silica concentrations compared to discharge temperature, low pH and high total carbonate. This situation has been described by Arnórsson (1985) as a chemical evidence of mixing. According to Arnórsson, the chemistry of mixed waters tends to be under-saturated with respect to calcite and is also characterized by lack of equilibrium with secondary minerals which is a characteristic feature of geothermal water. Looking at Figure 13, it is evident that thermal springs in the study area have been affected by mixing.

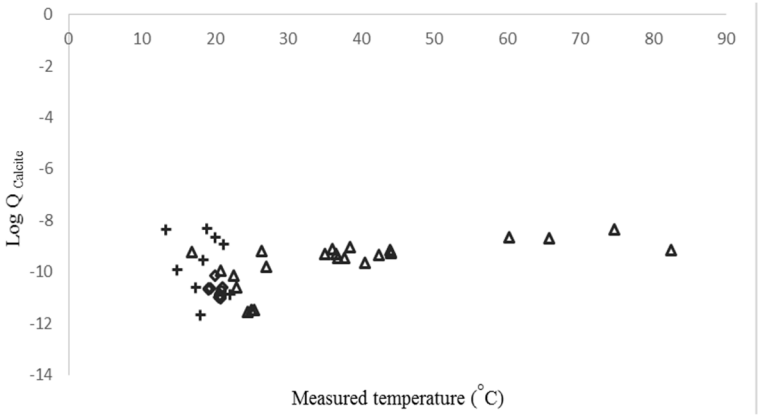

FIGURE 13: The state of calcite saturation relative to sampling temperatures in the Ngozi geothermal field. Diamond shapes represent lake water, triangles spring water and crosses river water

The modification to the model described by Björke et al. (2015) and Stefánsson et al. (2016) was made because some of the thermal spring with low discharge temperature indicate higher SiO_2 concentration (Figure 6) and chalcedony geothermometry temperature (Figure 14) than springs with higher discharge temperature. This was thought to be the result of cooling upon mixing with cold non-thermal waters because the concentration of SiO_2 is directly proportional to temperature.

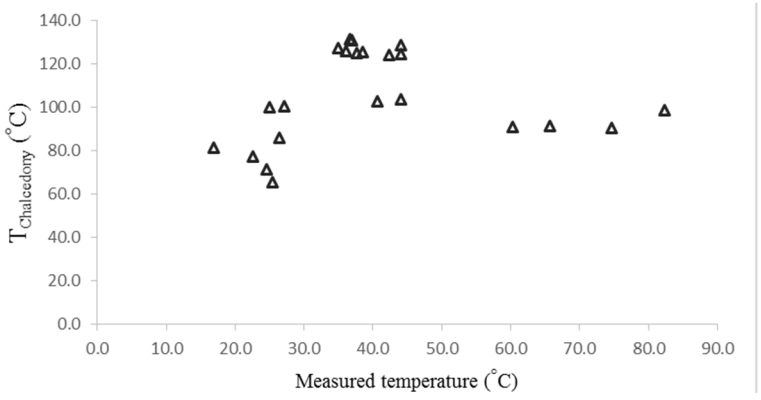

FIGURE 14: Chalcedony geothermometry relative to measured temperature for thermal spring waters in the study area

According to Fournier (1977) and Arnórsson (2000) the dissolved silica in most natural waters is not affected by common ion effect, formation of complexes and loss of volatile components. For this reason, silica can be regarded as a conservative upon mixing and chloride has also been considered to be non-

reactive upon mixing and tend to remain in solution and do not enter into the secondary minerals structure (Mahon, 1970; Stefánsson et al., 2016).

The mixing modelling results (Table 2) indicate that thermal springs close to the Ngozi volcano are generally not mixed with lake water. Songwe spring shows about 13% mixing with lake water however the structural setting in the area limits this possibility due to the presence of bounding fault between two described in section 2.2 of this study. Therefore, its slight similarity with lake water can be explained by an interaction with rocks with similar chemistry. Ibayi and Udindilwa springs display about 7% and 5% mixing with lake water respectively and are the only thermal springs in the area that can be postulated to have a relationship with the lake. However thermal springs display varying degrees of dilution by non-thermal waters in the area where most springs are heavily mixed while some are moderately mixed. Only Inyala, Iyela and Aqua-Afia springs show insignificant mixing with non-thermal waters.

Most rivers also do not show mixing with lake water. However, Igogwe, Kiwira, Gogozimba and Kwamana rivers display about 16.5%, 2.6%, 1.8% and 1.5% mixing with lake water, respectively. This implies that these rivers are draining Lake Ngozi water in the subsurface because the lake has no surface outlet. In the Ngozi geothermal field most rivers show mixing with thermal springs water in the area of varying degrees (Table 2; Figure 15 and 16). Only Mbalizi and Mchewe rivers shows no mixing with thermal spring waters while Songwe River shows insignificant mixing with thermal spring waters.

4.5 Water-rock interactions

The chemistry of geothermal water is not only modified by mixing, depressurization boiling or conductive heat loss during ascent to the surface, but also by water rock interaction (Björke et al., 2015, Stefánsson et al., 2016). Water-rock interaction leads to alteration of rock, hence formation of alteration mineralogy, as well as to increased concentration of rock forming elements in geothermal water especially when the flow rate of the spring is not high enough. Auko (2014) pointed out that water-rock interaction can be viewed as an acid-base reaction where water containing dissolved gasses act as acid while the rock forming minerals act as base and they react to a stable or metastable secondary minerals. As seen in Table 3 and Figure 6, most of the thermal springs are enriched with rock forming elements like SiO_2, Na, K, Ca and Mg. In the study area, there are few alteration minerals identified as discussed in section 2.5 of this study probably due to thick cover of pyroclastic ash as discussed in section 2.2 of this study. However, the intensity of surface activities like alteration can be limited by mixing described in the section 4.4 above and limited residence time of fluids.

From Figure 17, it can be noted that the waters have been interacting with Na-Al silicates and Ca-Al silicates, which belong to the zeolites group of minerals, with Na-Ca-Al-Mg silicates belonging to smectite group of minerals and with silica bearing rocks. Because most of the thermal spring waters are super saturated with respect to Na-Al mineral analcime, all the waters are super saturated with respect to chalcedony. Lake water is saturated with respect to Ca-Al minerals and montmorillonites while thermal springs and rivers are generally super saturated with respect to Ca-Al minerals and montmorillonites. The observation that waters in the study area have been interacting with zeolites, minerals of the smectite-group and silica bearing rocks is in agreement with secondary mineral assemblage identified in the area as described in part 2.5 of this study.

Some river waters in the study area which are considered non-thermal waters are enriched with rock forming elements and hence saturated and/or super saturated with respect to the secondary minerals. This is in agreement with the mixing calculation which shows that most rivers are significantly mixed with thermal spring waters hence it can be concluded that the concentration of rock forming elements like Si, Na, K, Ca and Mg is controlled by water-rock interaction.

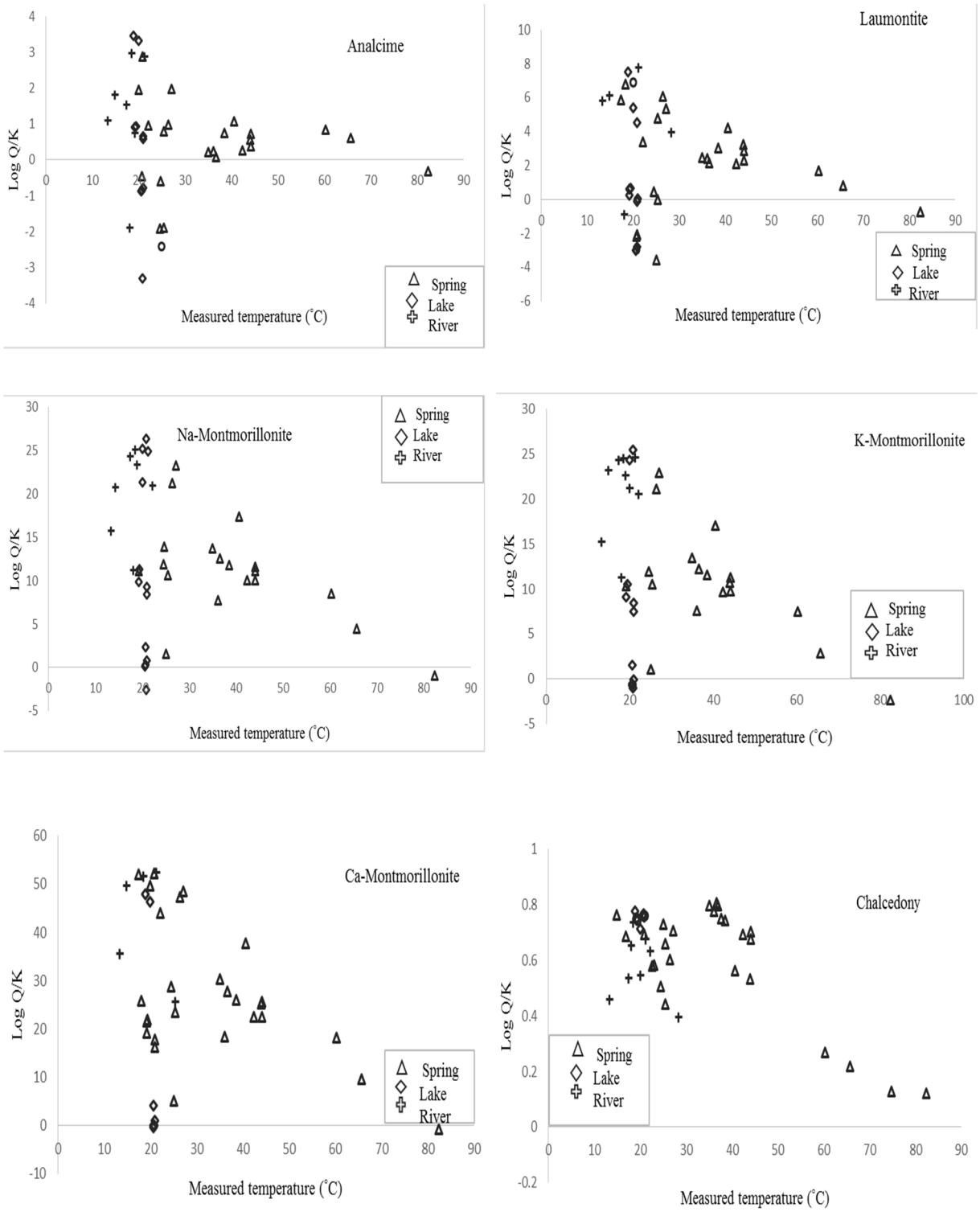

FIGURE 17: Saturation state of waters in the Ngozi geothermal field with respect to secondary minerals

5. CONCLUSIONS

The waters of different types (thermal springs, rivers and lake waters) in the Ngozi geothermal field were studied. Geothermometry temperatures for selected springs were estimated using the multiple equilibrium technique and other solute geothermometers. The results of geothermometry shows that the maximum temperatures to be expected in the subsurface of thermal springs around Ngozi volcano is 120-130°C. From these results, it can be concluded that the thermal springs around the Ngozi volcano maybe fed by meteoric water percolating to the subsurface through permeable structures and get heated up. After attaining reasonable temperatures and becoming less dense, the water rises to the surface as thermal springs in the fairly shallow circulation (Figure 18).

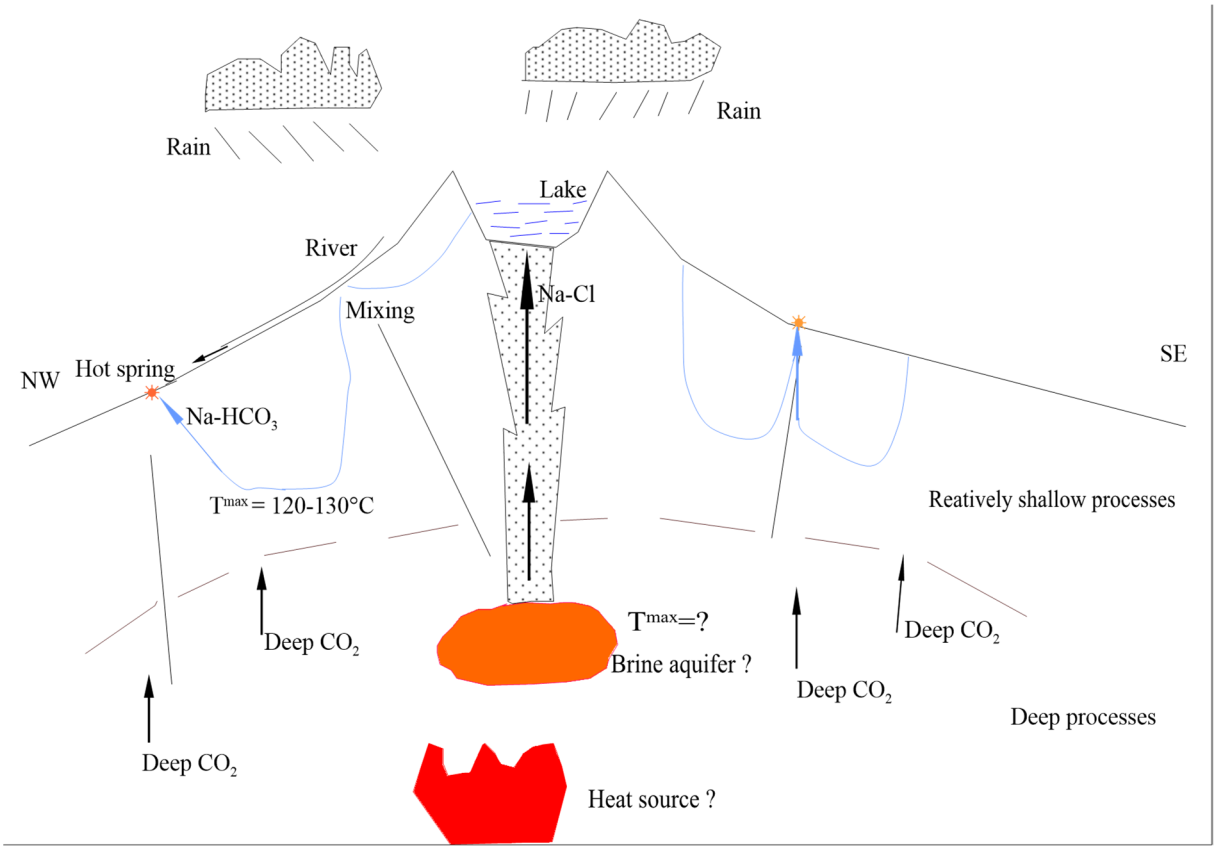

FIGURE 18: Conceptual model of the processes controlling water chemistry in the Ngozi geothermal field

Considering the EC values of the springs it can be concluded that the springs have had relatively low residence time that was not enough to dissolve much ions from the rocks. The idea of shallow circulation is also supported by very low concentration of volcanic gases like HCl and H_2S in some of the studied springs. For these springs, the source of HCO_3 fluids can be explained as a result of dissolution of carbonate bearing rocks in the shallow depth as evidenced by Ilamba, Manyogopa and Mbete springs which are characterized by Ca (Mg) - HCO_3 composition which was thought to be a result of calcite dissolution.

Mixing between the lake, thermal springs and river waters was quantified based on the model developed and described by Björke (2015) and Stefánsson (2016) with little modification. The results show that some rivers including Igogwe, Kiwira, Gogozimba and Kwamana contain lake water in the order of 16.5%, 2.6%, 1.8% and 1.5% respectively while other rivers do not show mixing with lake water. However, most rivers show mixing with thermal spring waters. On the other hand, thermal springs show insignificant to no mixing with lake water but significant mixing with non-thermal water. The chemistry

of thermal spring waters and rivers mixed with thermal spring waters shows that the concentration of main rock forming elements are controlled by water-rock interaction and these waters have been interacting with zeolites, smectite and silica bearing minerals.

The cold gas vents in the area can be interpreted as a result of deep degassing and transport to surface. Why this gas is cold can be explained in two ways: firstly, the gas cools by expansion when leaving the magma body towards the surface, and the second possibility is that this gas interacts on its ascent with groundwater aquifers and cools before reaching the surface.

ACKNOWLEDGEMENTS

I would like to thank the UNU-GTP and the government of Iceland at large for giving me the opportunity to attend the six months course in Chemistry of Thermal Fluids. My gratitude also goes to my company, Tanzania Geothermal Development Company Limited for granting me time to attend this course.

My appreciation also goes to all staffs of UNU-GTP; Mr. Lúdvík S. Georgsson, Mr. Ingimar G. Haraldsson, Ms. Þórhildur Ísberg, Mr. Markús A. G Wilde and Ms. Málfríður Ómarsdóttir for their generous support and care they have been providing when needed throughout the training. Staff of ÍSOR and all lecturers are appreciated for their support and/or transferring their knowledge and experience during lectures and other meetings also Ms. Rósa S. Jónsdóttir for proving the references whenever required. UNU Fellows for the year 2016 are also appreciated for their various support. My landlady during my time in Iceland Ms. Þórkatla Jónsdóttir is also appreciated.

I am also thankful to my final project supervisor Prof. Andri Stefánsson of Faculty of Earth Sciences, University of Iceland, for his patience and guidance throughout preparation of this work. The knowledge gained from him is highly appreciated and will help me further in my career. Mr. Finnbogi Óskarsson and Halldór Ármannsson are also appreciated for always having time for discussion whenever requested.

I also thank Almighty God for his grace and mercy that kept me safe and healthy throughout the training. Last but not least, my heart felt gratitude is to my lovely wife and my family who have been supporting me in different ways throughout the course.

REFERENCES

Arnórsson, S., 1985: The use of mixing models and chemical geothermometers for estimating underground temperature in geothermal systems. *J. Volc. Geotherm. Res., 23,* 299-335.

Arnórsson, S. (ed.), 2000: *Isotopic and chemical techniques in geothermal exploration, development and use. Sampling methods, data handling, interpretation*. International Atomic Energy Agency, Vienna, 351 pp.

Auko, L.O., 2014: Evaluation of fluid-mineral interaction in the Menengai geothermal syatem, Central Rift, Kenya. Report 8 in*: Geothermal training in Iceland 2014.* UNU-GTP, Iceland, 39-64.

Bjarnason, J.Ö., 2010: *The chemical speciation program WATCH, version 2.4*. ÍSOR – Iceland GeoSurvey, Reykjavik, website: *www.geothermal.is/software.*

Björke, J. K., Stefánsson, A. and Arnórsson, S., 2015: Surface water chemistry at Torfajökull, Iceland – Quantification of boiling, mixing, oxidation and water-rock interaction and reconstruction of reservoir fluid composition. *Geothermics, 58,* 75-86.

de Moor, J.M., Fischer, T.P., Sharp, Z. D., Hilton, D.R., Barry, P.H., Mangasini, F., and Ramirez C., 2012: Gas chemistry and nitrogen isotope compositions of cold mantle gases from Rungwe Volcanic Province, southern Tanzania. *Chemical Geology, 339,* 30-42.

Delalande, M.M., Bergonzini, L., Gherardi,, F., Guidi, M., Andre, L., Abdallah, I. and Williamson, D., 2011: Fluid geochemistry of natural manifestations from the southern Poroto-Rungwe hydrothermal system (Tanzania): Preliminary conceptual model. *J. Volc. Geotherm. Res., 199*, 127-141

Delalande, M.M., Gherardi, F., Williamson, D., Kajula, S., Kraml, M., Noret, A., Abdallah, I., Mwandapile, E., Massault, M., Majule, A., and Bergonzini, L., 2015: Hydrogeochemical features of Lake Ngozi (SW Tanzania). *J. African Earth Sciences, 103*, 153-167.

Delvaux, D., Kraml, M., Sierralta, M., Wittenberg, A., Mayalla, J. W., Kabaka, K., Makene, C and GEOTHERM working group, 2010: Surface exploration of a viable geothermal resource in Mbeya area, SW-Tanzania. Part I: Geology of the Ngozi –Songwe geothermal system. *Proceedings of the World Geothermal Congress 2010. Bali, Indonesia*, 7 pp.

Ebinger, C.J., Deino, A.L., Drake, R.E and Tesha, A.L., 1989: Chronology of volcanism and rift basin propagation: Rungwe Volcanic province, East Africa. *J. Geophys. Res., 94* 15,785-15,803.

Fontijn, K., Delvaux, D., Ernst, G.G.J., Kervyn, M., Mbede, E., and Jacobs, P., 2010a: Tectonic control over active volcanism at a range of scales: Case of the Rungwe volcanic province, SW Tanzania; and hazard implications. *J. African Earth Sciences, 58*, 764-777.

Fontijn, K., Ernst, G.G.J., Elburg, M.A., Williamson, D., Abdallah, E., Kwelwa, S., Mbede, E., and Jacobs, P., 2010b: Holocene explosive eruption in the Rungwe volcanic province, Tanzania. *J. Volc. Geoth. Res., 196,* 91-110.

Fontijn, K., Williamson, D., Mbede, E. and Ernst, G.G.J., 2012: The Rungwe volcanic province, Tanzania – a review. *J. African Earth Sciences, 63*, 12-31.

Fournier, R.O., 1977: Chemical geothermometers and mixing model for geothermal systems. *Geothermics, 5,* 41-50.

Fournier, R.O., and Potter, R.W. II, 1979: Magnesium correction to the Na-K-Ca geothermometer. *Geochim. Cosmochim. Acta, 43,* 1543-1550.

Fournier, R.O., and Potter, R.W. II, 1982: A revised and expanded silica (quartz) geothermometer. *Geoth. Res. Council Bull.,11-10*, 3-12.

Giggenbach, W.F., 1986: Graphical techniques for the evaluated water/rock equilibration conditions by use of Na, K, Mg and Ca contents of discharge water. *Proceedings of the 8th New Zealand Geothermal Workshop, Auckland, NZ,* 37-43.

Kalberkamp, U., Schaumann, G., Ndonde, P.B., Chiragwile, S.A., Mwano, J.M and GEOTHERM Working Group, 2010: Surface exploration of a viable geothermal resource in Mbeya area, SW Tanzania. Part III: Geophysics. *Proceedings of the World Geothermal Congress 2010. Bali, Indonesia,* 6 pp.

Kraml, M., Mnjokava, T.T., Mayalla, J.W., Kabaka, K., and GEOTHERM Working Group., 2010: Surface exploration of a viable geothermal resource in Mbeya area, SW Tanzania. Part II: Geochemistry. *Proceedings of the World Geothermal Congress 2010. Bali, Indonesia,* 8 pp.

Mahon, W.A.J., 1970: Chemistry in the exploration and exploitation of hydrothermal systems. *Geothermics, Sp. issue 2-2,* 1310-1322.

Marini, L., Chiodini, G., and Cioci, R., 1986: New geothermometers for carbonate-evaporite geothermal reservoir. *Geothermics, 15-1*, 77-86.

Nicholson, K., 1993: *Geothermal fluids: chemistry and exploration techniques*. Springer-Verlag, Berlin, 268 pp.

Njue, L., 2015: Geothermal manifestations. *Presented at "Short Course X on Exploration for Geothermal Resources", UNU-GTP, KenGen and GDC, Lake Naivasha, Kenya*, UNU-GTP SC-21, 17 pp.

Ochmann, N., and Garofalo, K., 2013: *Geothermal energy as an alternative source of energy for Tanzania*. GEOTHERM Project, final technical report, 156 pp.

Parkhurst, D.L., and Appelo, C.A.J., 2015: *Description of input and examples for PHREEQC, version 3 - A computer program for speciation, bath-reaction, one-dimensional transport, and inverse geochemical calculations*. USGS, USA, computer software.

Reed, M.H., and Spycher, N.F., 1983: Calculated pH at high temperature in hydrothermal waters with application to geothermometry. *Paper presented at 4th Internat. Symposium on Water-Rock Interaction, Extended Abstracts*, 401-404.

Reed, M.H., and Spycher, N.F., 1984: Calculation of pH and mineral equilibria in hydrothermal water with application to geothermometry and studies of boiling and dilution. *Geochim. Cosmochim. Acta, 48*, 1479-1490.

Stefánsson, A., Keller, N.S., Robin, J.G., Kaasalainen, H., Björnsdóttir, S., Pétursdóttir, S., Jóhannesson, H., and Hreggvidsson, G.O., 2016: Quantifying mixing, boiling, degassing, oxidation and reactivity of thermal waters at Vonarskard, Iceland. *J. Volcanology and Geothermal Res., 309,* 53-62.

TGDC and GDC, 2015: *Geological and structural mapping of Ngozi geothermal field*. Tanzania Geothermal Development Company, Ltd., and Geothermal Development Company, Ltd., Kenya, report of field mapping.

Truesdell, A.H., and Fournier, R.O., 1977: Procedure for estimating the temperature of a hot water component in a mixed water using a plot of dissolved silica vs. enthalpy. *US Geol. Survey, J. Res., 5,* 49-52.